A Structural Account of Substrate and Inhibitor Specificity Differences between Two Naphthol Reductases‡

Der-Ing Liao,*,§ James E. Thompson,||,⊥ Stephen Fahnestock,§ Barbara Valent,@ and Douglas B. Jordan*,#

Experimental Station, DuPont Central Research and Development, Wilmington, Delaware 19880, Stine-Haskell Research Center, DuPont Agricultural Products, Newark, Delaware 19704, Experimental Station, DuPont Agricultural Products, Wilmington, Delaware 19880, and Experimental Station, DuPont Pharmaceuticals Company, Route 141 and Henry Clay Road, Wilmington, Delaware 19880-0357

Received April 10, 2001; Revised Manuscript Received May 31, 2001

ABSTRACT: Two short chain dehydrogenase/reductases mediate naphthol reduction reactions in fungal melanin biosynthesis. An X-ray structure of 1,3,6,8-tetrahydroxynaphthalene reductase (4HNR) complexed with NADPH and pyroquilon was determined for examining substrate and inhibitor specificities that differ from those of 1,3,8-trihydroxynaphthalene reductase (3HNR). The 1.5 Å resolution structure allows for comparisons with the 1.7 Å resolution structure of 3HNR complexed with the same ligands. The sequences of the two proteins are 46% identical, and they have the same fold. The 30-fold lower affinity of the 4HNR−NADPH complex for pyroquilon (a commercial fungicide that targets 3HNR) in comparison to that of the 3HNR−NADPH complex can be explained by unfavorable interactions between the anionic carboxyl group of the C-terminal Ile282 of 4HNR and CH and CH_2 groups of the inhibitor that are countered by favorable inhibitor interactions with 3HNR. 1,3,8-Trihydroxynaphthalene (3HN) and 1,3,6,8-tetrahydroxynaphthalene (4HN) were modeled onto the cyclic structure of pyroquilon in the 4HNR−NADPH−pyroquilon complex to examine the 300-fold preference of the enzyme for 4HN over 3HN. The models suggest that the C-terminal carboxyl group of Ile282 has a favorable hydrogen bonding interaction with the C6 hydroxyl group of 4HN and an unfavorable interaction with the C6 CH group of 3HN. Models of 3HN and 4HN in the 3HNR active site suggest a favorable interaction of the sulfur atom of the C-terminal Met283 with the C6 CH group of 3HN and an unfavorable one with the C6 hydroxyl group of 4HN, accounting for the 4-fold difference in substrate specificities. Thus, the C-terminal residues of the two naphthol reductase are determinants of inhibitor and substrate specificities.

1,3,6,8-Tetrahydroxynaphthalene reductase (4HNR)[1] is a newly discovered enzyme from *Magnaporthe grisea* that operates in the fungal melanin biosynthetic pathway (Figure 1) (*1*). The enzyme and its sibling, 1,3,8-trihydroxynaphthalene reductase (3HNR), of the same pathway are typical short chain dehydrogenase/reductases (SDR), a superfamily of enzymes known for shared structural motifs and the diversity of its substrates (*2*, *3*). *M. grisea* is the causal agent of blast disease in rice, and it requires fungal melanin, a polymer of 1,8-dihydroxynaphthalene, for infection of host cells (*4*−*6*). Beginning with 1,3,6,8-tetrahydroxynaphthalene, the biosynthetic pathway in *M. grisea* proceeds through two alternating reduction and dehydration steps to yield 1,8-dihydroxynaphthalene. 3HNR is the physiological target of the commercial blasticides phthalide, pyroquilon, and tricyclazole (Figure 1), which bind in the naphthol pocket of the 3HNR active site (*7*−*9*). From more than two decades in practice, millions of pounds of these compounds have been applied to rice paddies for controlling the disease. Efforts to discover more efficacious inhibitors of the enzyme are reported (*9*−*11*). There is a single gene encoding the dehydratase of the pathway, known as scytalone dehydratase (SD),

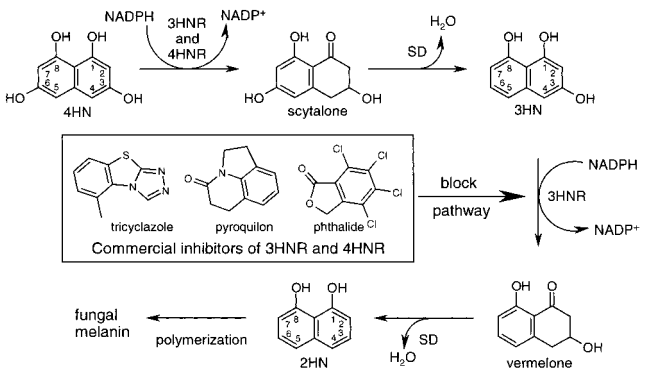

FIGURE 1: Fungal-melanin biosynthesis. 3HNR is the physiological target of the inhibitors.

‡ Atomic coordinates of the 4HNR−NADPH−pyroquilon complex have been deposited in the Protein Data Bank as entry 1JA9.

* To whom correspondence should be addressed. D. B. Jordan. Telephone: (*302*) 695−4280. Fax: (*302*) 695−4507. E-mail: doug.b.jordan@dupontpharma.com. D.-I. Liao. Telephone: (*302*) 695−8332. Fax: (*302*) 695−1351. E-Mail: der-ing.liao@usa.dupont.com.

§ DuPont Central Research and Development.

|| DuPont Agricultural Products, Newark.

⊥ Present address: Merck & Co., P.O. Box 2000, Rahway, NJ 07023.

@ DuPont Agricultural Products, Wilmington.

DuPont Pharmaceuticals Company.

[1] Abbreviations: 4HNR, 1,3,6,8-tetrahydroxynaphthalene reductase; 3HNR, 1,3,8-trihydroxynaphthalene reductases; 2HN, 1,8-dihydroxynaphthalene; 3HN, 1,3,8-trihydroxynaphthalene; 4HN, 1,3,6,8-tetrahydroxynaphthalene; SD, scytalone dehydratase; SDR, short chain dehydrogenase/reductases; Tris, tris(hydroxymethyl)aminomethane; HEPES, *N*-(2-hydroxyethyl)piperazine-*N*′-2-ethanesulfonic acid.

10.1021/bi0107243 CCC: $20.00
Published on Web 07/07/2001

which efficiently catalyzes the dehydration of scytalone and vermelone (*12*−*16*). SD is the physiological target of blasticides that have recently been commercialized (*17*−*18*) or are in development (*19*−*26*).

Genetic evidence prompted the discovery of 4HNR (*1*). *M. grisea* mutants lacking 3HNR accumulate 3HN (and its oxidation products), and double mutants lacking 3HNR and SD accumulate scytalone (Figure 1). The phenotypes of the mutants led to the hypotheses that either there is another reductase for mediating the conversion of 4HN to scytalone or there is another route to scytalone altogether in *M. grisea*. The problem was resolved by cloning the gene for the other reductase (4HNR) that encodes a protein that is 46% identical in sequence to 3HNR. Double mutants of *M. grisea* that lack 3HNR and 4HNR accumulate 4HN (and its oxidation products), thus indicating that 4HN is the sole source of scytalone and validating the pathway shown in Figure 1. *M. grisea* mutants lacking 4HNR have wild-type phenotypes and produce fungal melanin.

Substrate specificities of the two enzymes for 3HN and 4HN account for the observed phenotypes in the mutants lacking 3HNR or 4HNR (*1*). According to the k_{cat}/K_m ratios, 3HNR prefers 3HN over 4HN by a factor of 4 and 4HNR prefers 4HN over 3HN by a factor of 300. Thus, in *M. grisea* mutants lacking 4HNR, 3HNR may catalyze the reduction of 3HN and 4HN, the latter substrate being only 4-fold less efficient than the former, and the mutant organism reflects a wild-type phenotype from its production of fungal melanin. In *M. grisea* mutants lacking 3HNR, 4HNR activity is sufficient to mediate the reduction of 4HN, but the 300-fold lower efficiency of the enzyme for 3HN precludes clearing of 3HN, which accumulates to produce the distinct phenotype of the mutant.

X-ray structures of 3HNR in the absence and presence of NADPH and inhibitors have been determined (*7*, *9*, *27*). 3HNR binds the inhibitors phthalide, pyroquilon, and tricyclazole with the following affinity progression: 3HNR−NADPH > 3HNR−$NADP^+$ > 3HNR. This is consistent with the view that the inhibitors mimic the hydride-accepting keto tautomer of the naphthol substrate (*8*, *9*). The *pro-S* hydrogen of NADPH (the hydrogen that is transferred to naphthol substrates as a hydride) is directed toward the inhibitors and, in the case of pyroquilon, toward its carbonyl carbon (*7*, *9*). The 1.7 Å resolution X-ray structure of 3HNR complexed with NADPH and pyroquilon provides a simple guide for docking substrates 3HN and 4HN into the active site (*9*). Doing so shows causes overlap between the van der Waals surfaces of the C6 hydroxyl group of 4HN (the hydroxyl is replaced with a hydrogen in 3HN) and the SD sulfur atom of Met283, an electrostatic repulsion that can account for the 4-fold preference of 3HNR for 3HN over 4HN (*9*). Met283 is the C-terminal residue of 3HNR, and its position changes rather little among the X-ray structures of 3HNR (*9*). Since the C-terminus of 4HNR is one residue shorter than 3HNR according to a sequence alignment, it was suggested that electrostatic repulsion between 4HN and the protein would be relieved (*9*). However, it was not lost upon us that the lack of electrostatic repulsion is not a particularly satisfying explanation for the 300-fold preference for 4HN over 3HN held by 4HNR, and we sought experimental guidance for the binding mode of naphthol substrates in the 4HNR active site. The naphthol substrates, 3HN and 4HN, are unsuitable for cocrystallization studies with the enzyme due to their propensity for oxidation and polymerization. Pyroquilon, a flat cyclic molecule containing a carbonyl group, is the best inhibitor in complex with 3HNR and NADPH for modeling the naphthol substrates (*9*), and so for this work, we have determined the X-ray structure of 4HNR complexed with NADPH and pyroquilon. From the high-resolution structure, we also hoped to gain insight into why the affinity of pyroquilon for the 4HNR−NADPH complex is 30-fold lower than that for the 3HNR−NADPH complex.

EXPERIMENTAL PROCEDURES

Crystallization. Crystals of the 4HNR−NADPH−pyroquilon complex were obtained by cocrystallization of 4HNR in the presence of 10 mM NADPH and 2 mM pyroquilon. Crystals of the 4HNR−NADPH−pyroquilon complex were grown at 4 °C by using the hanging-drop diffusion method with 1.5 M Li_2SO_4 and 0.1 M HEPES-NaOH (pH 7.4) in the wells, a condition optimized from the Hampton Screen 1, Condition 16 (Hampton Research). A mixture of 1 μL of the protein/inhibitor solution [20 mg of protein/mL, 10 mM NADPH, 2 mM pyroquilon, and 50 mM Tris-HCl (pH 7.0)] and 1 μL of the well solution were contained in the hanging drops. Small crystals (0.02 mm × 0.05 mm × 0.1 mm) appeared after a few days, and they were stable for a few weeks. Larger crystals were obtained by adjusting the salt concentration; however, invariably the larger crystals failed to diffract as well as the small crystals. Seeding studies were not attempted. Immediately prior to data collection, crystals were washed briefly in a solution of 1.6 M Li_2SO_4, 0.1 M HEPES-NaOH (pH 7.4), and 20% glycerol, mounted on nylon loops with a diameter of 0.05−0.1 mm, and directly frozen in a nitrogen cold stream at −170 °C.

Data Collection. 4HNR crystals were too small to produce a diffraction pattern by using our in-house X-ray source produced by a Rigaku rotating anode generator with MSC focusing mirrors. A 2.5 Å data set from a single crystal was collected at the Brookhaven X12B synchrotron beam line using an ADSC Quantum 4 CCD detector. Data were processed by using the DENZO-SCALEPACK package (*28*). The crystal was tetragonal in space group $P4_22_12$ with the following cell dimensions: $a = b = 95.5$ Å and $c = 71.8$ Å. There is one molecule in the asymmetric unit, and the solvent content of the crystal is 40%. Subsequently, a 1.5 Å data set was collected from a single crystal at the Argonne Advanced Photon Source, sector 5, insertion-device beam line using a MAR CCD detector. This data set was processed in a manner similar to that of the first and used for the final refinement of the structure. The data collection statistics are listed in Table 1.

Structure Determination. Molecular replacement was carried out with the program AMoRe from the CCP4 program suite (*29*). Residues 25−283 of the refined model of the 3HNR−NADPH−pyroquilon complex (PDB entry 1GO0) were used as the searching model with NADPH, the inhibitor, and the side chains other than the Cβ atoms eliminated. The electron density map, calculated using the phase information from the molecular replacement solution, was displayed, and models of the side chains were built by using a Silicon Graphics system and the program O (*30*). NADPH and

Table 1: Data Collection and Refinement Statistics[a]

Data Collection			
wavelength (Å)	0.963	no. of unique reflections	51109
resolution (Å)	30−1.5	completeness (%)	97.5 (71.6)
space group	$P4_22_12$	R_{merge} (%)	7.9 (38.1)
cell dimensions (Å)	94.8, 94.8, 71.2	no. of molecules per asymmetric unit	1
no. of observations	487876	water content (%)	40
Refinement			
resolution (Å)	6.0−1.5	rmsd for bond angles (deg)	1.53
R_{work}	0.189	no. of non-hydrogen atoms	1889
R_{free}	0.221	no. of water molecules	218
rmsd for bond lengths (Å)	0.012		

[a] Values are for the data set collected using a single crystal at the Argonne Advanced Photon Source. Values in parentheses refer to the highest-resolution shell (1.53−1.50 Å).

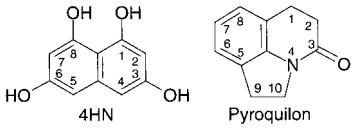

FIGURE 2: Molecular modeling by the numbers. In the 4HNR−NADPH−pyroquilon complex, pyroquilon atoms were changed to those of 4HN according to the numbering system that guides an overlay of the two molecules.

pyroquilon were incorporated into the model after one run of molecular dynamics refinement by using the slow-cool protocol of XPLOR (*31*). A portion of the data (10%) was omitted from the refinements for the purpose of calculating R_{free} (*32*). With the X12B data set, the model was refined to a final working R value of 20.8% and an R_{free} value (*32*) of 31.5%, without the addition of water molecules. This model was then refined against the high-resolution APS-5ID data set. Refinement statistics for the final model are listed in Table 1.

Other Methods. The *M. grisea* 4HNR was heterologously overexpressed in *Escherichia coli* and purified to homogeneity as described previously (*1*). Pyroquilon was modified to 4HN in the 4HNR−NADPH−pyroquilon complex by using the Build/Edit function of the modeling package Sybyl (Tripos, Inc.) and the numbering system of Figure 2 to overlay the substrate onto the inhibitor. The nicotinamide rings of NADPH in the 3HNR−NADPH−pyroquilon and 4HNR−NADPH−pyroquilon complexes were overlaid upon one another by using the Fit Atoms function in Sybyl. Figures 3, 4, and 6 were generated using the program RIBBONS (*33*).

RESULTS

Overall Structure of Tetrahydroxynaphthalene Reductase. The three-dimensional structure of 4HNR complexed with NADPH and pyroquilon was determined by using molecular replacement methods and the protein coordinates of the 3HNR−NADPH−pyroquilon complex (PDB entry 1GO0) (*9*). Even though the single crystal of the 4HNR−NADPH−pyroquilon complex used for data collection was quite small, with synchrotron radiation coupled to an undulator it diffracted to 1.5 Å resolution. The electron density map provides excellent definition of most of the protein, including the inhibitor, NADPH, and residues of the active site (Figure 3a). Good statistics for data collection and refinement were obtained (Table 1). For the convenience of making comparisons with 3HNR, which has an N-terminus that is eight residues longer than that of 4HNR in the alignment, the numbering of 4HNR begins with residue 9. The model includes residues 24−282, lacking assignments for the first 15 residues, which includes the N-terminal Met-Ala dyad, which is removed upon production of 4HNR in *E. coli* (*1*). The electron density is clearly incompatible with an Ile at position 231 as assigned from the nucleotide sequence. Resequencing (three times) of the DNA indicates a Met residue at position 231, which agrees with the electron density, and Met231 is assigned in the PDB file.[2] 4HNR has the same fold as 3HNR, and an rms difference of 0.95 Å results from an overlay of Cα atoms of 4HNR and 3HNR. The asymmetric unit contains a single subunit of 4HNR, and after four of these have been merged, it is clear that 4HNR likely exists as a homotetramer with 222 symmetry (Figure 3b) as does 3HNR (*7*, *9*). The binding mode of NADPH is similar in the 3HNR and 4HNR structures. The structural motif (Gly-X-X-X-Gly-X-Gly) shared by SDR members for discriminating between NADP(H) and NAD(H) forms of the dinucleotide substrates is perfectly conserved between 3HNR and 4HNR (Gly36-Ala37-Gly38-Arg39-Gly40-Ile41-Gly42), and the residues occupy similar space relative to the 2′-phosphate of NADPH in the two structures. The structural motif commonly found in SDR members for mediating catalysis (Tyr-X-X-X-Lys) is Tyr178-Ser179-Gly180-Ser181-Lys182 in 3HNR and Tyr178-Ala179-Gly180-Ser181-Lys182 in 4HNR. In both 3HNR and 4HNR, residues 178−182 form a loop with the two end residues (Tyr178 and Lys182) constituting part of the proposed proton shuttling route in 3HNR (*9*) and 4HNR (see Catalysis).

Inhibitor Binding. The electron density allows for an unambiguous assignment of the orientation of pyroquilon in the 4HNR active site (Figure 3a). Likewise, the electron density of the inhibitor in the 3HNR−NADPH−pyroquilon complex provides a clear assignment (see the Supporting Information for a figure showing the electron density surrounding pyroquilon in the 3HNR−NADPH−pyroquilon complex). In comparison to the orientation in the 3HNR−NADPH−pyroquilon complex, pyroquilon is upside down in the 4HNR−NADPH−pyroquilon complex. That is, when the nicotinamide rings of the NADPH molecules of the 3HNR−NADPH−pyroquilon and 4HNR−NADPH−pyroquilon complexes are overlaid, the pyroquilon molecules are at 180° with respect to one another, pivoted about the inhibitor's carbonyl oxygen atom (Figure 4a). The two orientations of pyroquilon with respect to the nicotinamide ring of NADPH in the 3HNR and 4HNR structures occupy similar space in the two active sites, and either inhibitor orientation can be accommodated in the 3HNR and 4HNR active sites without severe steric conflicts with protein residues.

Many of the inhibitor interactions in the new structure are reminiscent of those seen in the 3HNR−NADPH−pyroquilon complex: the hydroxyl groups of Ser164 and Tyr178

[2] The corrected nucleotide sequence has been reported to the GenBank.

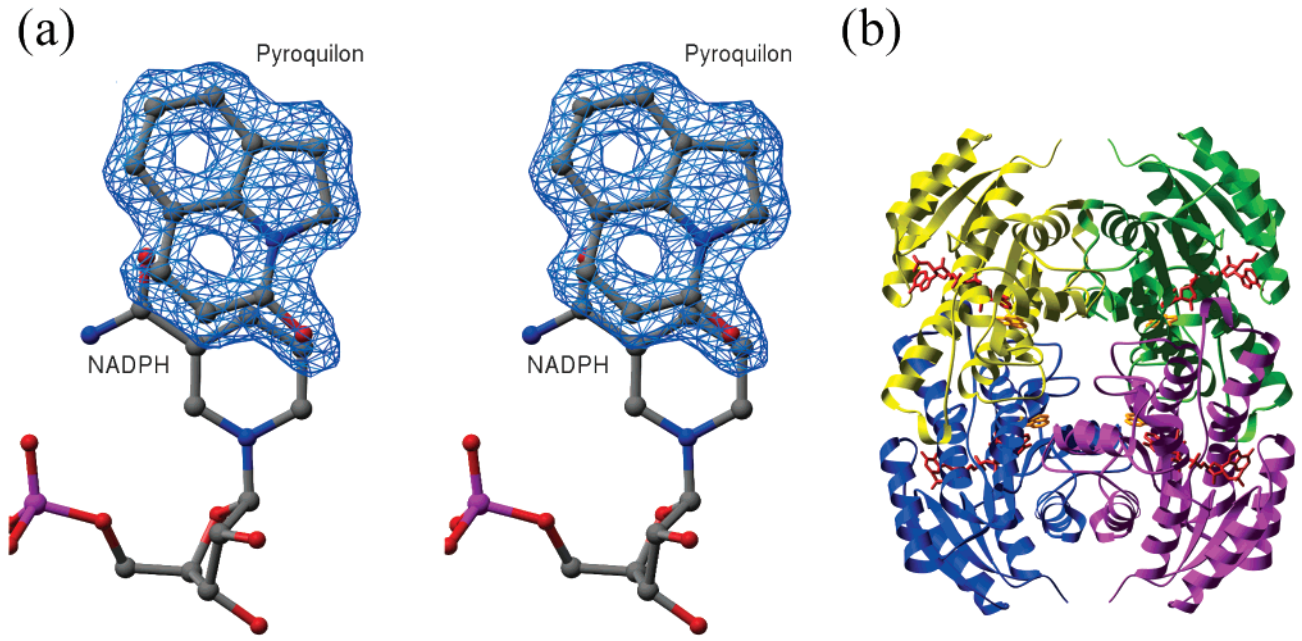

FIGURE 3: Structure of tetrahydroxynaphthalene reductase. (a) Stereoview of the $F_o - F_c$ omit map of pyroquilon in the active site of 4HNR. The map is contoured at 3.5σ. (b) The homotetramer of tetrahydroxynaphthalene reductase.

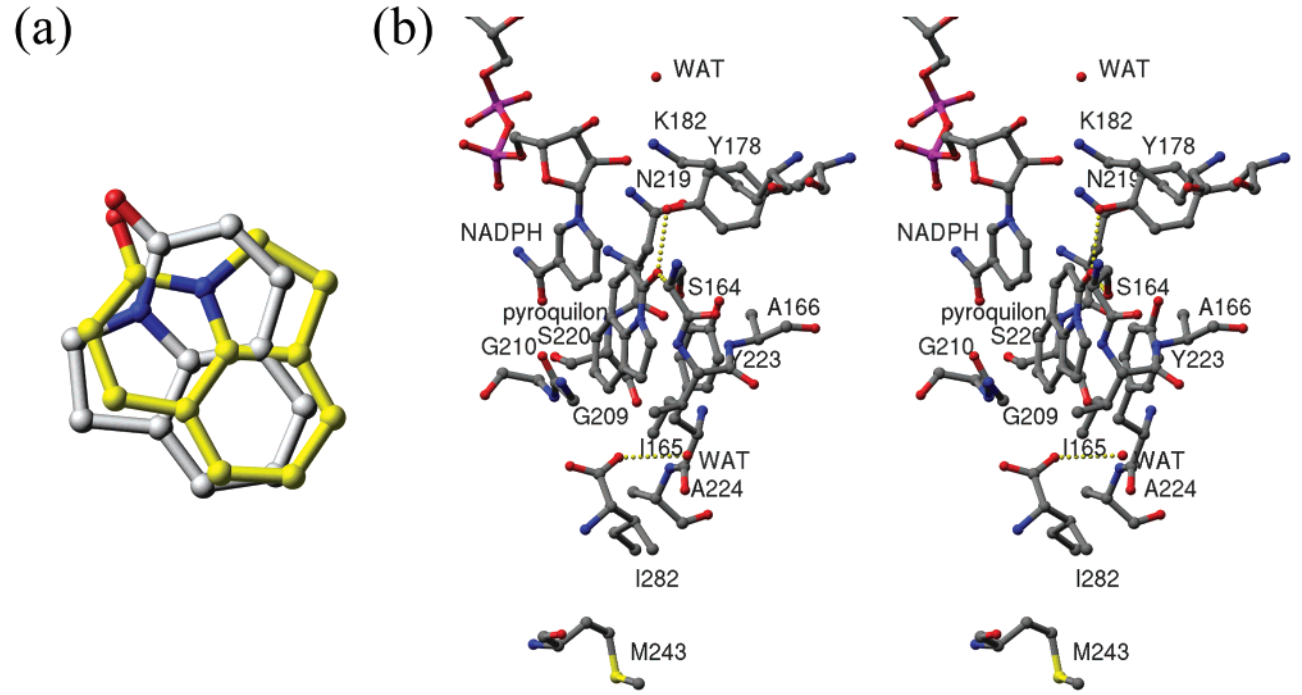

FIGURE 4: Binding of pyroquilon by the 4HNR−NADPH and 3HNR−NADPH species. (a) The relative orientations of pyroquilon in the 4HNR−NADPH−pyroquilon and 3HNR−NADPH−pyroquilon structures. The nicotinamide rings of the two structures were overlaid to obtain the relative orientations of pyroquilon. Pyroquilon from the 4HNR structure has gray carbon atoms and C−C bonds. Pyroquilon from the 3HNR structure has yellow carbon atoms and C−C bonds. The electron density maps provide unambiguous assignments for pyroquilon in the 4HNR−NADPH−pyroquilon structure (Figure 3a) and the 3HNR−NADPH−pyroquilon structure (Supporting Information). (b) Stereoview of the pyroquilon binding pocket in the 4HNR−NADPH−pyroquilon complex. WAT denotes a crystallographic water molecule. Dotted lines represent hydrogen bonds.

are hydrogen bonded to the inhibitor's carbonyl oxygen, the ring of Tyr223 is stacked with the inhibitor's ring system, the *pro-S* hydrogen atom of NADPH is directed toward the inhibitor's carbonyl carbon, and hydrophobic interactions are provided by several residues (Figure 4b). Within a 4 Å sphere surrounding the inhibitor of the 4HNR−NADPH−pyroquilon complex are elements of 16 protein residues. Eight residues (Ser164, Ile165, Tyr178, Pro208, Gly209, Gly210, Met215, and Tyr223) are conserved in 3HNR, and eight 4HNR residues are replaced in 3HNR as follows: Glu118Val, Ala166Thr, Met169Ala, Phe216Tyr, Asn219Val, Ser220Cys, Leu240Ala, and Ile282Cys. The Glu118Val replacement, perhaps the most dramatic change, is softened because the side chains point in different directions and away from the inhibitor. The hydrogen bond between the carboxyl group of Glu118 and the hydroxyl group of Tyr223 in 4HNR is

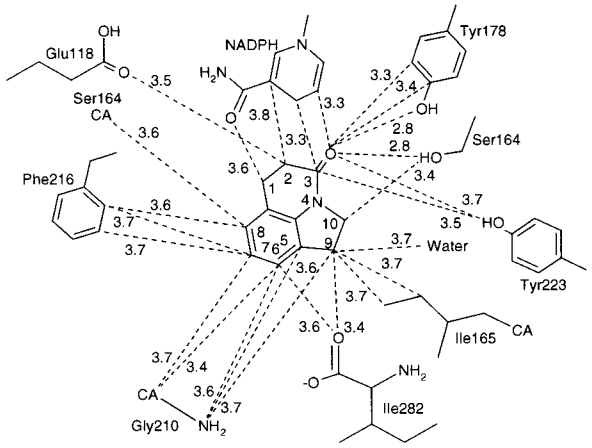

FIGURE 5: Schematic of pyroquilon contacts in the 4HNR−NADPH−pyroquilon complex. Contacts within a 3.8 Å radius of the inhibitor (hydrogen atoms not included) are indicated. Distances between non-hydrogen atoms are in angstroms. The numbering system for pyroquilon atoms of Figure 2 is used. For simplicity of presentation, several interactions with the ring atoms of Tyr223 are not indicated. Compare with the schematics of pyroquilon contacts in the 3HNR−NADPH−pyroquilon complex (Figure 4 of ref *9* and Supporting Information).

replaced by a hydrogen bond between the imidazole group of His175 and the hydroxyl group of Tyr223 in 3HNR.

A schematic shows that within a 3.8 Å radius of the inhibitor are numerous contacts between 4HNR residues and pyroquilon (Figure 5). There are about twice as many contacts than are seen in the 3HNR−NADPH−pyroquilon complex (see Figure 4 of ref *9* and the Supporting Information for schematic views of pyroquilon contacts in the 3HNR−NADPH−pyroquilon complex). However, the K_i value for the 4HNR−NADPH−pyroquilon complex (420 nM) is 30-fold larger than that of the 3HNR−NADPH−pyroquilon complex (14 nM) (*1*). In both the 3HNR−NADPH−pyroquilon and 4HNR−NADPH−pyroquilon structures, the inhibitor is covered well by the protein. However, in the 4HNR structure, there is a crystallographic water molecule held next to a methylene group of pyroquilon (the water molecule is hydrogen bonded to the carboxyl group of Ile282), whereas in the 3HNR structure, there is no crystallographic water near pyroquilon nor is there room for one (see Figure 3 of ref *9*). The space of the crystallographic water of 4HNR is occupied by the sulfur atom of Met283 in 3HNR. Thus, the desolvation energies of the inhibitor are expected to be more beneficial to binding in the 3HNR complex than in the 4HNR complex.

Additional contributions to the differences in the affinities of 3HNR and 4HNR for pyroquilon arise from the respective C-terminal residues and their inhibitor contacts. In the 4HNR−NADPH−pyroquilon complex, the carboxyl group of Ile282 is near the C6 CH and C9 CH_2 groups of the inhibitor (Figure 5). The Ile282 carboxyl group is near crystallographic water molecules, so it is expected to be in an anionic form that would have an unfavorable interaction with the inhibitor. If the orientation of pyroquilon in the 3HNR−NADPH−pyroquilon complex is placed into the 4HNR active site, the carboxyl group of Ile282 is located near a different CH group (C8) of the inhibitor (4.0 Å between the oxygen and carbon atoms). The CH interaction with the carboxyl group may be even less favorable than the one with the CH_2 group; certainly, the CH group mimics an interaction with 3HN against which the enzyme selects (see Substrate Specificities). In the case of the 3HNR−NADPH−pyroquilon complex, the S8 sulfur atom of Met283 is nearest to the C1 CH_2 group of the inhibitor (4.2 Å between the carbon and sulfur atoms). If the orientation of pyroquilon in the 4HNR−NADPH−pyroquilon complex is placed into the 3HNR active site, the S8 sulfur atom becomes close to a different methylene group (C9) of the inhibitor (3.7 Å between the carbon and sulfur atoms). In this orientation, the van der Waals radii of the S8 sulfur atom and the C9 CH_2 group of pyroquilon are in contact, perhaps accounting for why 3HNR selects against it and favors the determined orientation (*9*).

Substrate Specificities. The structure of 4HN was mapped onto that of pyroquilon of the 3HNR−NADPH−pyroquilon structure to provide a view of the naphthol in the 3HNR active site (*9*). As pyroquilon has a different disposition in the 4HNR active site, a modified method for mapping the atoms of 4HN onto those of the inhibitor was employed (Figure 2) that results in the 4HNR−NADPH−4HN model shown in Figure 6a. This method places 4HN in the active site of 4HNR in a position similar to that obtained when 4HN is transferred from its docked position in the 3HNR model (*9*) by overlaying the nicotinamide ring atoms of NADPH in both structures (see the Supporting Information for a figure showing the model of the 4HNR−NADPH−4HN complex obtained by this method). Alternatively, when 4HN is transferred from our model of the 4HNR−NADPH−4HN complex to the 3HNR−NADPH complex by overlaying the NADPH atoms, the position of 4HN in the 3HNR active site (Figure 6b) is similar to that provided by the previous model obtained by the other method (see Figure 5 of ref *9*). In essence, the two methods of docking 3HN and 4HN into the 3HNR and 4HNR active sites that are based on the positions of pyroquilon in the 3HNR−NADPH−pyroquilon and 4HNR−NADPH−pyroquilon X-ray structures, respectively, produce similar models implicating the C-terminal residues of 3HNR and 4HNR and the C6 substitutions of the naphthol substrates in roles of deciding whether 3HN or 4HN is preferred.

Models of 4HN complexed with the 4HNR−NADPH species predict that there is a hydrogen bond formed between the C-terminal carboxyl group of 4HNR (Ile282) and the C6 hydroxyl group of 4HN, providing a favorable binding interaction (Figure 6a and Supporting Information). The carboxyl group of Ile282 is partially exposed to solvent (and near crystallographic water molecules), meaning it likely exists in an anionic form which would have a favorable binding interaction with the hydroxyl group of 4HN but an unfavorable one with the position 6 CH group of 3HN. In addition, it is conceivable that the carboxyl group of Ile282 could produce a nonproductive binding complex with 3HN by hydrogen bonding to the C3 hydroxyl group, thus preventing access of C3 of 3HN to the *pro-S* hydrogen of NADPH.

When our model of the 4HNR−NADPH−4HN complex is used to position 4HN in the structure of the 3HNR−NADPH−pyroquilon complex, the resulting 3HNR model shows that the van der Waals radii of the oxygen atom of the 4HN C6 hydroxyl group and the S8 sulfur atom of Met283 of 3HNR are in contact, which would result in an

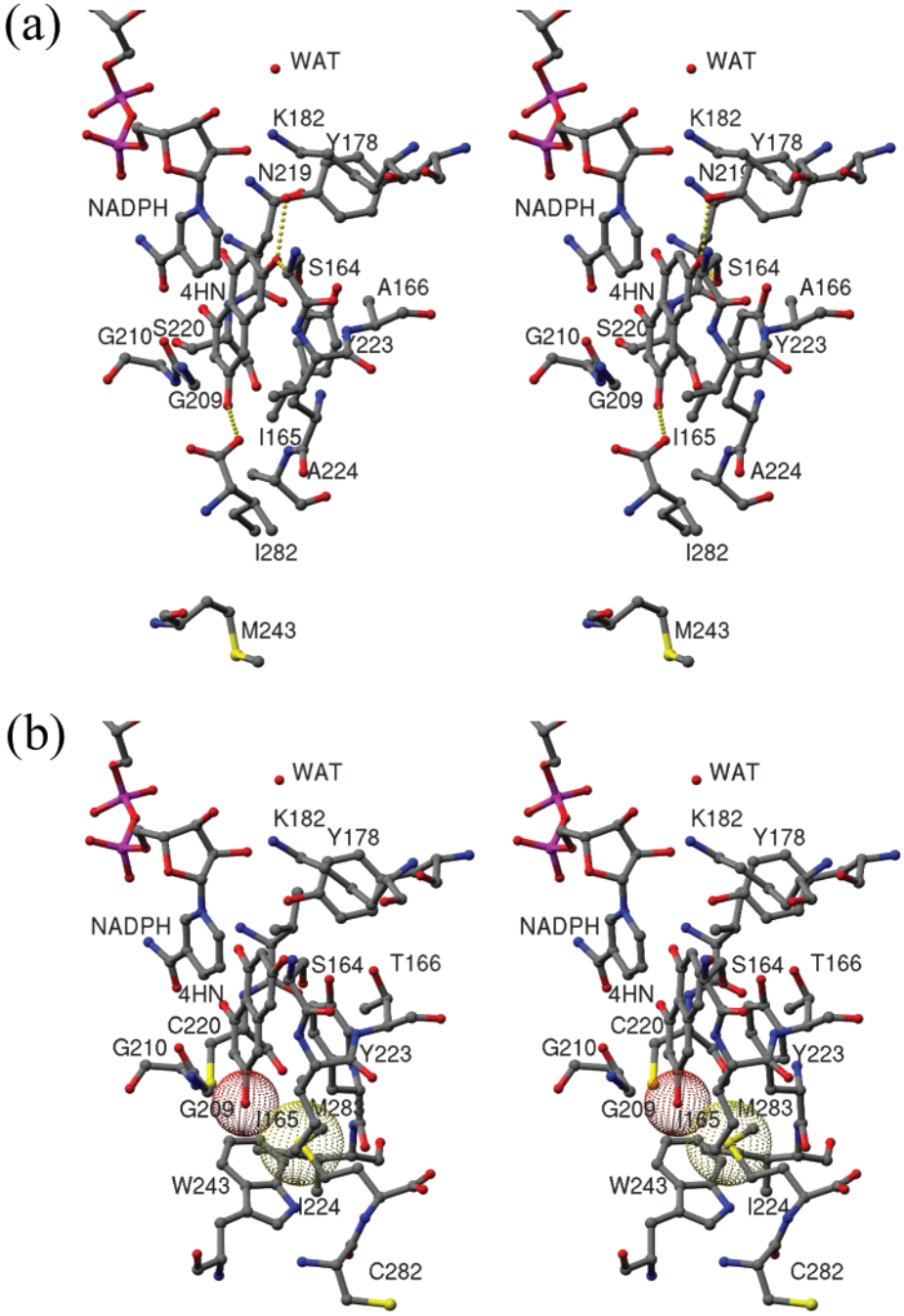

FIGURE 6: Docking of 4HN into the active sites of 4HNR and 3HNR. (a) Stereoview of the modeled 4HNR−NADPH−4HN complex obtained from the 4HNR−NADPH−pyroquilon complex with pyroquilon transformed to 4HN as described in the legend of Figure 2. Dotted lines represent hydrogen bonds. (b) Stereoview of the modeled 3HNR−NADPH−4HN complex obtained by transferring 4HN from its orientation with respect to the nicotinamide ring of NADPH in the 4HNR−NADPH−4HN model of panel a to the 3HNR−NADPH−pyroquilon structure maintaining the orientation of 4HN with respect to the nicotinamide ring of 3HNR and removing pyroquilon from 3HNR. The van der Waals surfaces of the C6 hydroxyl oxygen of 4HN and the S8 sulfur atom of Met283 are shown.

unfavorable electrostatic interaction (Figure 6b). The 3HNR−NADPH−4HN model prepared by the method of mapping 4HN onto the structure of pyroquilon in the 3HNR−NADPH−pyroquilon structure shows overlap between the van der Waals surfaces surrounding the S8 sulfur atom of Met283 and the C6 hydroxyl group oxygen atom of 4HN (*9*), similarly suggesting an unfavorable interaction between 4HN and the protein but with a greater degree of severity. In both of our models, the C6 CH group of 3HN is directed toward the sulfur atom of Met283 of 3HNR, producing an attraction or, at least, not an unfavorable interaction.

Catalysis. 3HNR and 4HNR have similar residues in place for promoting the reduction of naphthols, so the catalytic cycles are likely similar. Unlike 3HN, in aqueous solution a significant portion of 4HN exists in keto form (*34*, *35*), the tautomer expected to accept the hydride. Like the model of 3HNR (*9*), 4HNR has hydroxyl groups of Ser164 and Tyr178 positioned to stabilize the 3-keto tautomer of the naphthol through hydrogen bonds to the carbonyl oxygen (Figure 7). The ring of Tyr223 is modeled as stacked with the 4HN naphthol ring on the face of the substrate opposite the nicotinamide ring of NADPH. Although it is modeled as

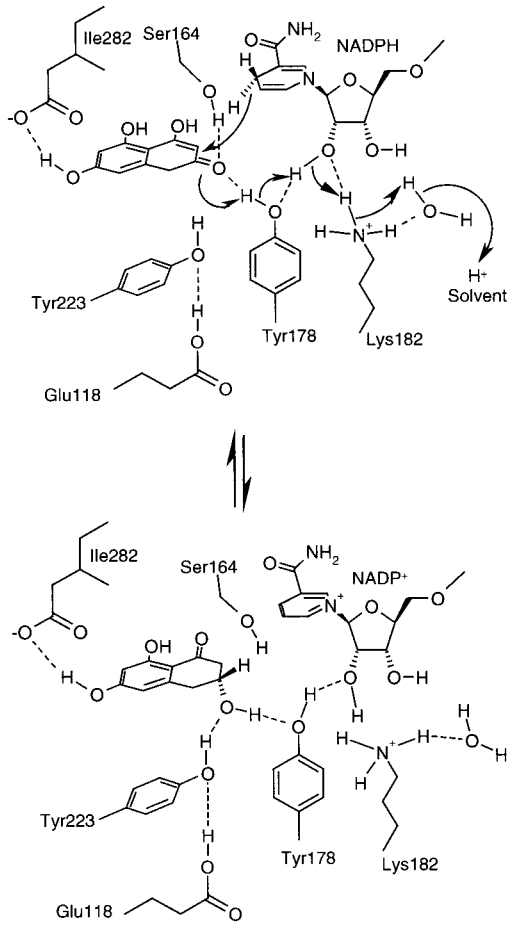

FIGURE 7: Proposed mechanism for the 4HNR-catalyzed reduction of 4HN to scytalone.

being too far away in the ground state (3.7 Å) to do so, in the transition state the hydroxyl group of Tyr223 may serve to hydrogen bond to the 3-keto oxygen atom of the naphthol substrate to assist in puckering the ring at C3 for approaching an ideal conformation for hydride acceptance. In promoting this function, the hydroxyl group of Tyr223 is hydrogen bonded to the carboxyl group of Glu118, which likely exists in neutral form because of the hydrophobic environment. The Glu118 carboxyl group is, in turn, hydrogen bonded to the imidazole group of His175. In 3HNR, the hydrogen bonding interaction of Tyr223 is with His175 whose imidazole group is also in a hydrophobic environment. In the 3HNR-catalyzed reaction, protonation of the substrate's carbonyl oxygen is proposed to occur through a proton shuttling mechanism that proceeds through the hydroxyl group of Tyr178, the 3′-hydroxyl group of NADPH, the NZ group of Lys182, and a crystallographic water molecule, the ultimate donor (*9*). All of these groups (including the crystallographic water molecule) are in place in the X-ray structure of the 4HNR−NADPH−pyroquilon complex. Similar to that in the 3HNR structure, the crystallographic water molecule in the 4HNR structure has a relatively low *B* factor of 13.2 Å^2 in comparison to the averaged *B* factors of the crystallographic water molecules (28.4 Å^2) and the protein atoms (13.9 Å^2). Taken together, this adds a measure of support for the proposed protonation route in the 3HNR mechanism and extends the proposal to the mechanism of 4HNR. Similar protonation routes are suggested by the X-ray structures of other SDR catalysts (*9*).

DISCUSSION

The high-resolution structure of the 4HNR−NADPH−pyroquilon complex complements the high-resolution structure of the 3HNR−NADPH−pyroquilon complex (*9*). Together they provide a unified view of enzyme-catalyzed reduction of naphthols, which includes stabilization of the keto tautomer of substrate, puckering of the ring system for hydride acceptance, and a proton shuttling route. Differences in the substrate specificities of 3HNR and 4HNR appear to reside in forces of electrostatic attractions and repulsions between the respective C-terminal residues and the C6 substitutions of the naphthol substrates. Such forces are common determinants of substrate specificities among enzymes, perhaps most widely known in dehydrogenases that discriminate between the 2′-substitutions of NAD(H) and NADP(H) forms of their substrates (*36*−*39*). Although there are some cases where substrate or cofactor recognition is through a C-terminal residue (*40*−*42*), the example presented in this work is the only known case where the C-terminal residues of two enzyme homologues are determinants of discrimination between alternate substrates. There is a 1300-fold difference in the relative substrate specificities for 3HN and 4HN between 3HNR and 4HNR (*1*). In perspective, however, the SDR family is rich with respect to the diversity of its substrates and has another example of substrate discrimination between enzyme homologues that is particularly relevant; i.e., the two tropinone reductases (64% identical in sequence with the same fold) catalyze the addition of hydride to the opposite faces of the substrate carbonyl group, producing opposite diastereomers of the alcohol (*43*). If pyroquilon were accepted as a substrate by 3HNR and 4HNR [it is not a substrate (*1*, *9*)], the products of the two enzyme-catalyzed reactions would have opposite stereochemistry because the *pro-S* hydrogen of NADPH is directed toward the opposite faces of the inhibitor carbonyl in the 3HNR−NADPH−pyroquilon and 4HNR−NADPH−pyroquilon structures.

Like their influences on the binding of 3HN, the influences of C-terminal residues of 3HNR and 4HNR on the binding of pyroquilon and likely the other two commercial fungicides of Figure 1 appear to be opposite. The S8 sulfur atom of Met283 has favorable interactions with the three fungicides according to the X-ray structures (*9*), whereas the carboxyl group of Ile282 has unfavorable interactions with the CH and CH_2 groups of pyroquilon. Apparently, the forces involving the two C-terminal residues that dictate discrimination between 3HN and 4HN are involved in determining inhibitor binding affinities. The physiological implication of the linkage between the dual roles of substrate and inhibitor recognition has practical significance; e.g., if 4HNR retained its lower affinities for the commercial fungicides but had equal substrate specificities for 3HN and 4HN, then it could provide a means of resisting the inhibitory effects of the compounds on the biosynthesis of fungal melanin in *M. grisea*, thus neutralizing the effectiveness of the fungicides shown in Figure 1.

Understanding the naphthol reductases of fungal melanin biosynthesis began with the realization that the rather simple heterocycles of commercial significance (Figure 1) operate by inhibiting the function of 3HNR in fungal cultures (*44*−*46*). Genetic analyses of fungal-melanin deficient mutants of *M. grisea* indicated that 3HNR is the product of a single

gene and suggested the presence of another reductase in the biosynthetic pathway that could mediate the reduction of 4HN to scytalone (*4*). The "other reductase" must have lower inhibitor affinities than 3HNR because the commercial inhibitors of 3HNR lead to the accumulation of 3HN and its byproducts rather than 4HN and its byproducts, the latter intermediate preceding the former according to the sequence of Figure 1. Adding mystery to the idea of different binding affinities was the report that tricyclazole was a noncompetitive inhibitor of 3HNR activity with respect to its naphthol substrate and the suggestion that the inhibitor binds in an allosteric site (*47*). Thereafter, the X-ray structure of the 3HNR−NADPH−tricyclazole complex was determined, and it strongly suggests that tricyclazole occupies the naphthol binding site (*7*), a finding that was sustained by a reevaluation of tricyclazole inhibition of 3HNR activity (*8*).

Occupation of the naphthol binding pocket by the inhibitors could suggest that 3HNR and the other reductase might have considerably different active site architectures to account for the effects of inhibitors and mutations on fungal-melanin biosynthesis in *M. grisea*. However, an alignment of the 3HNR and 4HNR sequences predicts that there are not major changes in the active sites of the two proteins (*1*). It could be envisioned that the C-terminus of 4HNR which is one residue shorter than that of 3HNR would accommodate 4HN better and weaken inhibitor binding, but this is an indirect effect according to the specific mechanisms supported by this work. Instead, it is apparent that the anionic C-terminal carboxyl group of 4HNR is involved in promoting the productive binding of 4HN over 3HN and compromising the binding of pyroquilon and that the C-terminal Met of 3HNR effects the opposite. In the end, differences of substrate and inhibitor affinities between 3HNR and 4HNR seem to boil down to the chemistry of their respective C-terminal residues, chemistry as simple as the commercial inhibitors that are responsible for bringing the proteins into known existence. The tales of the two naphthol reductases (including mode of inhibitor action, genetic, and enzymology studies) elaborate on the properties of the (C-terminal) tails of the two naphthol reductases.

ACKNOWLEDGMENT

This is DuPont CR&D contribution 8188.

SUPPORTING INFORMATION AVAILABLE

Figures showing the electron density defining the orientation of pyroquilon in the 3HNR active site, a schematic representation of the contacts between pyroquilon and 3HNR from the 3HNR−NADPH−pyroquilon structure, and the orientation of 4HN in the 4HNR active site as modeled from the modeled orientation of 4HN in the 3HNR active site. This material is available free of charge via the Internet at http://pubs.acs.org.

REFERENCES

1. Thompson, J. E., Fahnestock, S., Liao, D.-I., Valent, B., and Jordan, D. B. (2000) *J. Biol. Chem. 275*, 34867−34872.
2. Jörnvall, H., Persson, B., Krook, M., Atrian, S., Gonzalez-Duarte, R., Jeffrey, J., and Ghosh, D. (1995) *Biochemistry 34*, 6003−6013.
3. Jörnvall, H., Hoog, J.-O., and Persson, B. (1999) *FEBS Lett. 445*, 261−264.
4. Chumley, F. G., and Valent, B. (1990) *Mol. Plant-Microbe Interact. 3*, 135−143.
5. Bell, A. A., and Wheeler, M. H. (1986) *Annu. Rev. Phytopath. 24*, 411−451.
6. Howard, R. J., and Valent, B. (1996) *Annu. Rev. Microbiol. 50*, 491−512.
7. Andersson, A., Jordan, D. B., Schneider, G., and Lindqvist, Y. (1996) *Structure 4*, 1161−1170.
8. Thompson, J. E., Basarab, G. S., Andersson, A., Lindqvist, Y., and Jordan, D. B. (1997) *Biochemistry 36*, 1852−1860.
9. Liao, D.-I., Basarab, G. S., Gatenby, A. A., Valent, B., and Jordan, D. B. (2001) *Structure 9*, 19−27.
10. Liao, D.-I., Basarab, G. S., Gatenby, A. A., and Jordan, D. B. (2000) *Bioorg. Med. Chem. Lett. 10*, 491−494.
11. Jordan, D. B., Basarab, G. S., Liao, D.-I., Johnson, W., Winzenberg, K., and Winkler, D. A. (2001) *J. Mol. Graphics Modell.* (in press).
12. Lundqvist, T., Rice, J., Hodge, C. N., Basarab, G. S., Pierce, J., and Lindqvist, Y. (1994) *Structure 2*, 937−944.
13. Basarab, G. S., Steffens, J. J., Wawrzak, Z., Schwartz, R. S., Lundqvist, T., and Jordan, D. B. (1999) *Biochemistry 38*, 6012−6024.
14. Jordan, D. B., Zheng, Y.-J., Locket, B. A., and Basarab, G. S. (2000) *Biochemistry 39*, 2276−2282.
15. Jordan, D. B., Basarab, G. S., Steffens, J. J., Schwartz, R. S., and Doughty, J. G. (2000) *Biochemistry 39*, 8593−8602.
16. Basarab, G. S., Jordan, D. B., and Zheng, Y.-J. (2000) *Org. Lett. 2*, 1541−1544.
17. Kurahashi, Y., Sakawa, S., Kinbara, T., Tanaka, K., and Kagabu, S. (1997) *Nippon Noyaku Gakkaishi 22*, 108−112.
18. Tsuji, G., Takeda, T., Furusawa, I., Horino, O., and Kubo, Y. (1997) *Pestic. Biochem. Physiol. 57*, 211−219.
19. *Agrow* (1997) Vol. 287, pp 21−22, PJB Publications Ltd., Richmond, UK.
20. Sieverding, E., Hirooka, T., Nishiguchi, T., Yamamoto, Y., Spadafora, V. J., and Hasui, H. (1998) in *Proceedings of the 1998 Brighton Conference—Pests and Diseases*, Vol. 2, pp 359−366, British Crop Protection Council, Brighton, England.
21. Chen, J. M., Xu, S. L., Wawrzak, Z., Basarab, G. S., and Jordan, D. B. (1998) *Biochemistry 37*, 17735−17744.
22. Jordan, D. B., Lessen, T., Wawrzak, Z., Bisaha, J. J., Gehret, T. C., Hansen, S. L., Schwartz, R. S., and Basarab, G. S. (1999) *Bioorg. Med. Chem. Lett. 9*, 1607−1612.
23. Basarab, G. S., Jordan, D. B., Gehret, T. C., Schwartz, R. S., and Wawrzak, Z. (1999) *Bioorg. Med. Chem. Lett. 9*, 1613−1618.
24. Wawrzak, Z., Sandalova, T., Steffens, J. J., Basarab, G. S., Lundqvist, T., Lindqvist, Y., and Jordan, D. B. (1999) *Proteins: Struct., Funct., Genet. 35*, 425−439.
25. Jennings, L. D., Wawrzak, Z., Amorose, D., Schwartz, R. S., and Jordan, D. B. (1999) *Bioorg. Med. Chem. Lett. 9*, 2509−2514.
26. Jennings, L. D., Rayner, D. R., Jordan, D. B., Okonya, J., Basarab, G. S., Amorose, D. K., Anacelerio, B. M., Gehret, T. C., Lee, J. K., Schwartz, R. S., and Whitmore, K. A. (2000) *Bioorg. Med. Chem. 8*, 897−907.
27. Andersson, A., Jordan, D., Schneider, G., and Lindqvist, Y. (1997) *FEBS Lett. 400*, 173−176.
28. Otwinowski, Z., and Minor, W. (1997) *Methods Enzymol. 276*, 307−326.
29. Navaza, J. (1994) *Acta Crystallogr. A50*, 157−163.
30. Jones, T. A., Zou, J.-Y., Cowan, S. W., and Kjeldgaard, M. (1991) *Acta Crystallogr. A47*, 110−119.
31. Brünger, A. T., Krukowski, J., and Erickson, J. (1990) *Acta Crystallogr. A46*, 585−593.
32. Brünger, A. T. (1992) *Nature 355*, 472−475.
33. Carson, M. (1997) *Methods Enzymol. 277*, 493−505.
34. Viviani, F., Gaudry, M., and Marquet, A. (1990) *J. Chem. Soc., Perkin Trans. 1*, 1255−1259.
35. Simpson, T. J., and Weerasooriya, M. K. B. (2000) *J. Chem. Soc., Perkin Trans. 1*, 2771−2775.
36. Rossmann, M. G., Liljas, A., Brändén, C.-I., and Banasak, L. J. (1975) in *The Enzymes* (Boyer, P. D., Ed.) 3rd ed., Vol. 11, pp 61−102, Academic Press, New York.

37. Wierenga, R. K., De Maeyer, M. C. H., and Hol, W. G. J. (1985) *Biochemistry 24*, 1346−1357.
38. Scrutton, N. S., Berry, A., and Perham, R. N. (1990) *Nature 343*, 38−43.
39. Chen, R., Greer, A., and Dean, A. M. (1996) *Proc. Natl. Acad. Sci. U.S.A. 93*, 12171−12176.
40. Minor, W., Steczko, J., Bolin, J. T., Otwinowski, Z., and Axelrod, B. (1993) *Biochemistry 32*, 6320−6323.
41. Perry, K. M., Carreras, C. W., Chang, L. C., Santi, D. V., and Stroud, R. M. (1993) *Biochemistry 32*, 7116−7125.
42. Guncar, G., Podobnik, M., Pungercar, J., Strukelj, B., Turk, V., and Turk, D. (1998) *Structure 6*, 51−61.
43. Nakajima, K., Yamashita, A., Akama, H., Nakatsu, T., Kato, H., Hashimoto, T., Oda, J., and Yamada, Y. (1998) *Proc. Natl. Acad. Sci. U.S.A. 95*, 4876−4881.
44. Tokousbalides, M. C., and Sisler, H. D. (1978) *Pestic. Biochem. Physiol. 8*, 26−32.
45. Woloshuk, C. P., Wolkow, P. M., and Sisler, H. D. (1981) *Pestic. Sci. 12*, 86−90.
46. Ishida, M., and Nambu, K. (1975) *Noyaku Kagaku 3*, 10−26.
47. Viviani, F., Vors, J. P., Gaudry, M., and Marquet, A. (1993) *Bull. Soc. Chem. Fr. 136*, 395−404.

BI0107243